

# 염료감응형 태양전지의 축전지로 사용되는 전기이중층콘덴서에 대한 연구

최진영<sup>1)</sup>, 이임근<sup>2)</sup>, 홍지태<sup>3)</sup>, 김희제<sup>4)</sup>

## Studies of electric double layer capacitors used for a storage battery of dye sensitized solar cell energy

Jinyoung Choi, Imgeun Lee, Jitae Hong, Heeje Kim

**Key words** : Dye-sensitized solar cell (DSC), Electric double layer capacitors (EDLC), Carbon, Charge behavior

**Abstract** : To design the effective usage of electric double layer capacitors (EDLCs) used for a storage device of dye sensitized solar cell(DSC) energy,we first investigated the accumulation state of electrical charges and the charge behavior in the EDLCs. Based on the results, the voltage characteristics of EDLCs connected to DSC energy were evaluated. The results showed that the charge accumulation region concentrated on central part of the carbonaceous electrode in EDLCs and the required times for charging and discharging were almost the same.

### 1. Introduce

Photovoltaic power generation [1] is a useful technique for the prevention of global warming and energy problems. However, the generation power is strongly influenced by the weather, and therefore the stable supply of the electric power is difficult. To use DSC energy efficiently, a storage battery that can deliver the stable electric power to the load is required. One of the widely accepted storage battery is the sealed lead-acid cell which has some superior properties such as a long life cycle and superiority in good power characteristic to size ratio. However, when the cell is under a remarkably cool condition, the electromotive force rapidly drops and then a higher replenishing voltage is required. In a warmer condition, the risk of overcharge becomes greater. In recent years, the fuel cells [2] have attracted much attention and demonstrated a good power capability nevertheless the response to the instantaneous power is relatively poor. Therefore, we examined to use an electric double layer capacitors (EDLCs)[3]~[7] operating as a storage device of some DSC energy.

EDLCs, in which the double-layer is formed at the interface between nanoporous carbonaceous electrode and nonaqueous electrolyte solution, have attracted special interest recently because of their

superior properties such as the high power density, the good cycle-ability and the speedy response for load fluctuations. The charge storage process due to the charge behavior influences such properties, i.e., the performance is not dominated by chemical reactions. Therefore, to optimize the EDLCs connected to DSCs, it is necessary to investigate the accumulation state of electrical charges and the charge behavior in the EDLCs.

In this study, measurements of the charge distributions in EDLCs were carried out during charging and discharging. Finally, the voltage characteristics of EDLCs connected to DSCs were examined.

### 2. Experiments and methods

Figure 1 shows the schematic drawing of EDLCs sample, which comprises two 400-mm-thick nanoporous carbonaceous electrodes mixed dielectric

1), 2), 3) 부산대 전기공학과

E-mail : dipper02@pusan.ac.kr

Tel : (051)510-2770 Fax : (051)513-0212

4) 부산대 전기공학과

E-mail : heeje@pusan.ac.kr

Tel : (051)510-2364 Fax : (051)513-0212

(polytetrafluoroethene PTFE) and carbon black. Carbon black and PTFE were mixed in a mass ratio of 17: 1: 2. The nonaqueous electrolyte was a mixed solution of propylene carbonate (PC) and tetraethylammonium tetrafluoroborate  $((C_2H_5)_4NBF_4)$  in a mol ratio of 1 : 4. Then, the total thickness of the EDLCs sample, which was composed of 5-layers, was 880  $\mu\text{m}$ . The Al-covered carbon layer was dried at 0.1 Torr (at 150°C) for 2h and was spot-welded in the required size (15 mm in diameter) as electrodes under Ar atmospheric pressure. Carbonaceous materials were characterized by applying the method of nitrogen adsorption. The BET (Brunauer, Emmett and Teller) total surface area, the total pore volume and the average pore diameter of the activated carbon were 2004  $\text{m}^2/\text{g}$ , 1.24  $\text{m}^3/\text{g}$  and 2.72 nm, respectively.

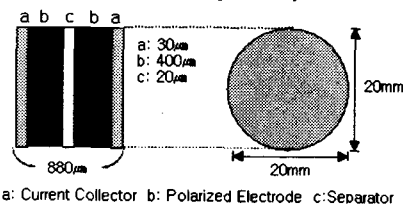


Fig.1 Schematic drawing of EDLC sample

The experimental arrangement for measurements of the charge distributions using a PEA system is shown in Fig. 2.

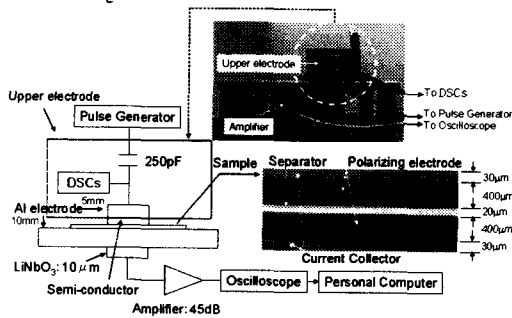


Fig. 2 Experimental arrangement using the PEA system

The principle of the PEA method is briefly outlined as follows: an electric pulse voltage together with a high DC voltage is added to EDLCs sample sandwiched between an upper and a lower electrode. Hence, acoustic waves are generated by the charges on the electrode and in the EDLCs sample. The acoustic waves propagate in both upper and lower directions, and they are converted into electric signals by a piezoelectric transducer arranged at the back of the lower electrode. The charge location can be determined by the response time of the electric signal, while the amount of charge is obtained from the magnitude of the signal. The voltage ( $V_{DC}$ ) of 2.5 V from a 1 DSC panel was added to EDLCs sample through an upper Al electrode 8 mm in diameter. The pulse voltage from a pulse generator had a maximum value of 600 V and a pulse width

of 2.5 ms at frequency of 400 Hz. Here, it is noted that a semiconductor layer was formed between the upper Al electrode and the EDLCs sample. The semiconductor layer adjusted the acoustic impedance on the interface between the EDLCs sample and the upper Al electrode. A 10- $\mu\text{m}$ -thick Lithium Niobate ( $\text{LiNbO}_3$ ) was used as a piezoelectric transducer. The transformed voltage signal was amplified 45 dB, and sent to a digital oscilloscope connected to a personal computer. The reflection of elastic waves on interfaces influences the interpretation of results in the case where PEA measurement is carried out on a sample constructed from some kinds of layers differing in acoustic characteristics, which is described in Sec. 3. We measured the charge distributions in EDLCs under various charging time ( $t_c$ ) of 0 - 20 s and discharging time ( $t_d$ ) of 0 - 20 s.

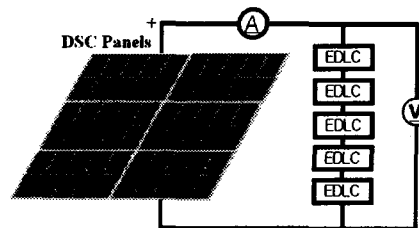


Fig. 3 Charging circuit of EDLC connected to 10 modules x 6 panels DSCs.

Figure 3 shows the charging circuit of EDLCs connected to DSCs. The number of EDLCs connected in series was 5, and their total capacitance was 500 F. They were connected to 10 modules x 6 panels DSCs with the output voltage of 12.5 V and the output power of 20 W.

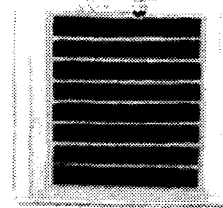


Fig. 4 Appearance of DSC

Figure 4 shows an appearance of DSC with photoelectric efficiency of 4% under solar-light source ( $\text{AM1.5}, 100\text{mW}/\text{cm}^2$ ). 1 DSC panel was fabricated by using 10 DSC parallel modules with similar performance. In the same way, five more panels were connected in parallel. In DSC panels connected in series and parallel, the output voltage of 12.5 V and the output current of about 1.6 A was obtained. Just after the electrification, the discharge characteristic of the EDLCs was examined by connecting a 20 W lamp to the EDLCs.

### 3. Results and discussions

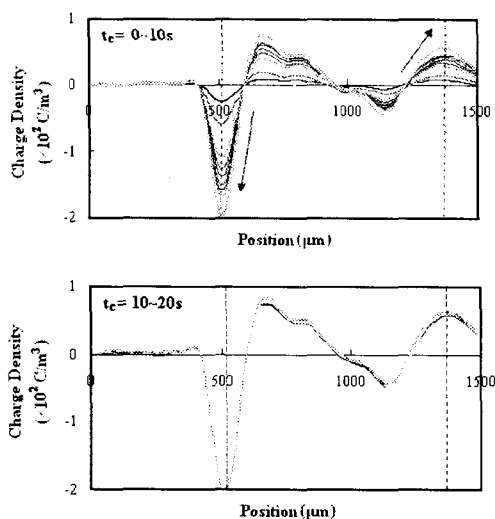


Fig. 5 Charge distributions obtained during charging.

The charge distributions in EDLCs, obtained during charging, are shown in Fig. 5. The transverse axis denotes the vertical distance ( $L$ ) from the upper Al electrode, i.e., the in-depth variation. The length, which is the distance between two vertical dotted lines, is equivalent to the thickness of EDLCs sample. It can be seen that the negative charge density was larger than the positive density. For example, the negative charge density obtained during charging had a maximum value of about  $205 \text{ C/m}^3$  near the collector layer (at  $L = 520 \text{ mm}$ ) while the positive charge density had a maximum value of about  $61.1 \text{ C/m}^3$  around the cathode layer (at  $L = 1400 \text{ mm}$ ). It is also noted that the polarized charge accumulation intensively occurred in the narrow region around porous carbon layer (at  $L = 520 - 1400 \text{ mm}$ ). The temporal variation of negative and positive charge densities with  $t_c$  is shown in Fig. 6.

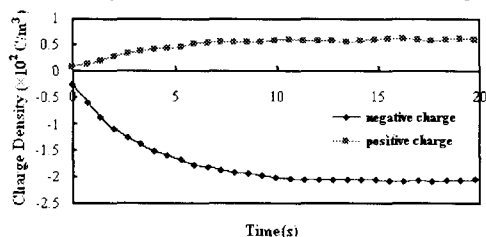


Fig. 6 Temporal variation of negative and positive charge densities with  $t_c$ .

Each plot denotes the absolute peak value of negative and positive peaks in the charge distribution and is the average of five measurements. It seems that the charge density increases as  $t_c$  increases and saturates at  $t_c > 10 \text{ s}$ . The charge distributions in EDLCs, obtained during discharging, are shown in Fig. 7.

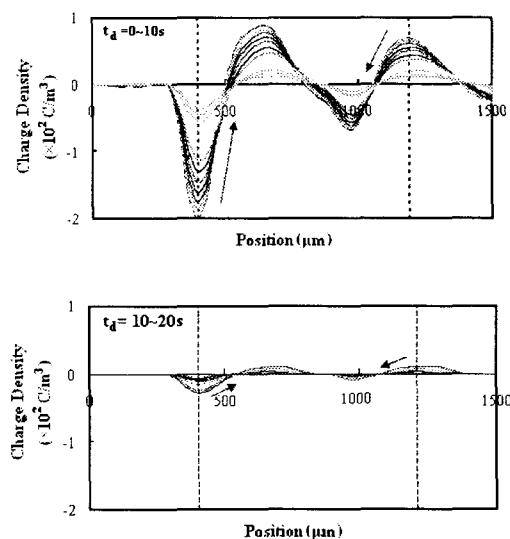


Fig. 7 Charge distributions obtained during discharging.

The remaining charge density gradually decays as  $t_d$  increases. The charge densities at  $t_d = 5, 10$  and  $20 \text{ s}$  are about  $-130, -36.0$  and  $-0.025 \text{ C/m}^3$ , respectively. Thus, the charging and the discharge process for EDLCs are almost achieved until  $t_c = t_d > 10 \text{ s}$ . Incidentally, the charge distributions shown in Figs. 5 and 7 suggest that the charge distribution in EDLCs is spatially uneven, i.e., hetero-charges distribution, which is presumed to be caused by the mobility of the positive and negative charges in the carbonaceous electrode surface of the EDLCs during the charging and the discharge. The charge mobility is closely concerned with the porous structure of the electrode materials, which did not change chemically during the charging and the discharging.

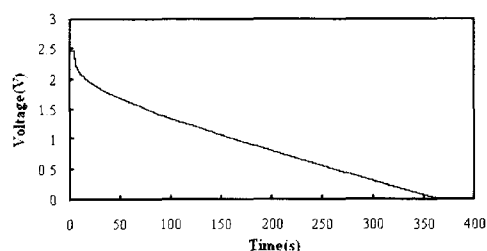


Fig. 8 . Example of oscilloscope trace of discharge voltage obtained from EDLC sample.

Incidentally, the electrostatic capacity of EDLCs is generally obtained by the energy conversion method. An example of oscilloscope trace of discharge voltage obtained from EDLCs sample is shown in Fig. 8.

The DSC with voltage of  $2.5 \text{ V}$  and the current density of  $5 \text{ mA/cm}^2$  was carried out in this experiment.

It seems that the discharge voltage curve contains two voltage drop components. A sudden

voltage drop ( $V_R$ ), which is associated with the internal resistive component, is seen at the beginning of discharge (400 ms).  $V_R$  was 0.3 V, which was equivalent to the current density of 5 mA/cm<sup>2</sup>. The capacitive component ( $V_{cap}$ ) is related to the voltage variation due to energy change in EDLCs. The capacitance ( $C_1$ ) per a sheet of carbonaceous electrode can be described as follows, using  $V_{cap}$  during the discharge.

$$C_1(F/g) = 2 \cdot \frac{i_d(A) \times \Delta t_d(s)}{m(g) \times \Delta V_{cap}(V)}$$

where  $i_d$  is the discharge current and  $m$  is the mass of the electrode made of activated carbon. The specific total capacitance ( $C_s$ ) in EDLCs can be calculated as  $C_s = 2C_1$  because two carbonaceous electrodes are in series arrangement. In the case of Fig. 8, it was calculated as  $C_s = 8.7$  F/g.  $C_s$  can also be estimated by the results of PEA measurements. The whole weight of two sheets of the carbonaceous electrodes was 140 mg, and the specific area of the electrodes was about 1625 m<sup>2</sup>/g. Adding up the charge density from  $L = 520$  to 1400 mm, the area charge density could be obtained. In the case of Fig. 5, the whole area charge density was calculated as  $8.92 \times 10^3$  C/m<sup>2</sup>.  $C_s$  could be estimated by dividing  $V_{DC}$  into the whole amount of electrical charges, and its value in the case of Fig. 5 was calculated as  $C_s = 9.36$  F/g. The values of  $C_s$ , obtained by two different methods, almost agreed within around 7%. When the PEA technique is performed on a sample constructed from some layers differing in acoustic characteristics, there is a possibility that the reflected elastic waves from the interfaces influence the interpretation of the experimental results. However,  $C_s$  obtained from the PEA method agreed well with that from the energy conversion method although the resulting  $C_s$  by the PEA method was estimated through an integration process of each charge distribution. This indicates that the PEA evaluation on  $C_s$  wasn't nearly affected by the component of reflected elastic waves. In our experimental conditions, two collectors were made of Al as with electrodes used in a PEA device. Even if the charge distributions reported here included some ambiguous factors due to reflected elastic waves, the ambiguity was not as large as that which didn't give physical meanings on the charge distribution. This enabled us to discuss the charge behavior using experimentally obtained results shown in Figs. 5 and 7.

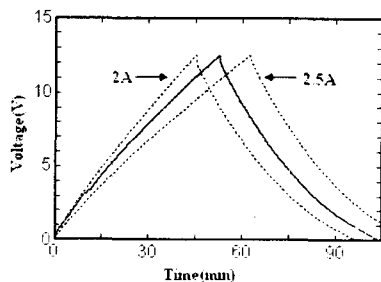


**Fig. 9 Voltage characteristics of EDLC connected to DSCs.**

Figure 9 shows the voltage characteristics of EDLCs connected to DSCs. The quantity of solar radiation was 100mW/cm<sup>2</sup>. The dotted lines denote the voltage change obtained using using DSCs whose total currents were set to 2 and 2.5 A, which are for indicating typical voltage characteristics for a stable power source. As can be seen from this figure, the required time for charging is almost the same as that for full discharging. This is consistent with the result obtained through measurements of charge distributions. Additionally, the efficiency of the output power against the input power was calculated as 98%.

#### 4. Conclusion

We first investigated the charge distributions in EDLCs in order to design the effective usage of the EDLCs used for a storage device of DSC energy. The charge distributions during charging and discharging were measured by means of a pulsed-electro-acoustic (PEA) method. The distributions of positive and negative charges were spatially uneven, which was due to the mobility of the positive and negative charges in the carbonaceous electrode surface of the EDLCs. It was also found that the voltage characteristics of EDLCs connected to DSCs was consistent with the result obtained through measurements of charge distributions and the required time for charging was almost the same as that for full discharging.

#### Acknowledgements

This work is partly supported by KOSEF(the Korea Science and Engineering Foundation) of Korea, grant No. R01-2004-000-10318-0.

#### References

- [1] L. Rosenblum, W. J. Bifano, G. F. Hein, A. F. Ratajczak, Solar Cells 1, pp. 65, 1979
- [2] R. Lemons, Journal of Power Sources 29, pp. 251, 1990
- [3] Brian. E. Conway "FElectrochemical Supercapacitors, NTS, 2001
- [4] M. Takeuchi, T. Maruyama, K. Koike, A. Mogami, T. Oyama and H. Kobayashi, Electro-chemistry 69, pp. 487, 2001
- [5] M. Okamura, H. Hasuike, M. Yamagishi and S. Araki, Electro-chemistry 69, pp. 414, 2001
- [6] Y. Kibi, T. Saito, M. Kurata, J. Tabuchi, A. Ochi: Journal of Power Sources 60, pp. 219, 1996
- [7] E. Lust, A. Janes, M. Arulepp, J. Solid State Electrochem 8, pp.488, 2004